Shikonin triggers GSDME-mediated pyroptosis in tumours by regulating autophagy via the ROS–MAPK14/p38α axis

Xiaoli Ju
Jiangsu University
Jiayou Wang
Jiangsu University
Jin Wang
Jiangsu University
Lanfang Guo
The Fourth People's Hospital of Jiangsu University
Heng Zhang
Nanjing Lishui District People's Hospital, Southeast University
Qiang Wang (wangqiang@ujs.edu.cn)
Jiangsu University

Research Article

Keywords: Shikonin, Pyroptosis, ROS, Autophagy, GSDME

Posted Date: June 7th, 2022

DOI: https://doi.org/10.21203/rs.3.rs-1659786/v1

Abstract

Shikonin (SK), a botanical drug extracted from *Lithospermum erythrorhizon*, has been shown to inhibit tumour growth through apoptosis and necrosis. However, whether SK induces pyroptosis in cancer cells is still unknown. Here, we demonstrated that SK treatment induced gasdermin E (GSDME)-dependent pyroptosis in tumour cells. The activation of BAX/caspase-3 signalling was essential for GSDME-mediated pyroptosis by SK. Mechanistically, the intracellular reactive oxygen species (ROS) generation induced by SK treatment initiated GSDME-dependent pyroptosis. SK stimulation induced protective autophagy in a ROS-dependent manner, and repressed autophagy significantly enhanced SK-induced pyroptosis. Moreover, MAPK14/p38α, a ROS sensor, modulated SK-induced autophagy and ultimately affected GSDME-dependent pyroptosis. This study demonstrated that SK initiates ROS signalling to drive pyroptosis in cancer cells and implicates SK as having an anticancer effect by inducing tumour cell death.

Introduction

The increase in intracellular reactive oxygen species (ROS) is closely related to the occurrence and development of cancer, and different ROS levels play a variety of roles in tumorigenesis [1]. Low levels of ROS promote tumour growth by promoting cancer cell proliferation and activating protumorigenic signalling and genomic instability. In contrast, and counterintuitively, ROS production can activate antitumourigenic signalling, leading to tumour cell death [2]. The activation of ROS can induce different types of cell death, such as apoptosis, necroptosis and ferroptosis, to inhibit tumour growth [3]. Accumulating data suggest that ROS are also involved in the activation of autophagy in tumour cells to protect against cell death [4, 5].

Pyroptosis is a type of inflammatory programmed cell death and can be divided into caspase-1-, caspase-11-, caspase-8- or caspase-3-dependent cell death depending on the activated caspases [6]. Recent studies have found that some chemotherapeutic drugs can induce tumour cell pyroptosis through the caspase-3 cleavage of gasdermin E (GSDME) [7, 8]. Many drugs, including natural extracts, have subsequently been found to induce pyroptosis in GSDME-expressing tumour cells [9–11]. Several studies have reported that intracellular ROS production induced by various stimuli can also regulate pyroptosis [12–14]. However, the detailed mechanism by which excessive ROS promotes pyroptosis is still unknown.

Shikonin (SK) is a botanical drug extracted from the root of *Lithospermum erythrorhizon*, an important herb in Chinese medicine [15]. Shikonin reportedly inhibits tumour growth in a variety of ways, such as inhibiting angiogenesis and inducing cell death [16]. However, no study has reported whether SK can inhibit tumour growth through the induction of tumour cell pyroptosis.

In the present study, we investigated the mechanism by which SK induces pyroptosis in vitro and in vivo. We found that SK induces GSDME-mediated pyroptosis in tumour cells. Furthermore, the activation of BAX/caspase-3 signalling is essential for the GSDME-mediated pyroptosis by SK. We also found that SK

stimulation can induce protective autophagy in tumour cells and that ROS production by SK stimulation regulated autophagy and ultimately affected GSDME-mediated pyroptosis. Further investigation revealed that MAPK14/p38α modulated ROS-dependent SK-induced pyroptosis and autophagy.

Materials And Methods

Cell lines and reagents

The human gastric cancer cell lines SGC-7901, BGC-823, and AGS were cultured in RPMI-1640 medium supplemented with 10% foetal bovine serum (FBS) and Pen/Strep (Gibco). HEK-293FT and the mouse cancer cell line EMT6 were cultured in Dulbecco's modified Eagle's medium (DMEM) supplemented with 10% FBS, and all cells were incubated with 5% CO_2 at 37 °C.

Antibodies and reagents

Antibodies and dilution ratio: anti-GSDME (Abcam, 1:1000); anti-caspase-3 (Sangon, 1:500); anti-BAX (CST, 1:1000); anti-LC3 (Sangon, 1:500); anti-GAPDH (Proteintech, 1:1000); anti-mouse IgG (Proteintech, 1:5000); anti-rabbit IgG (Sangon, 1:5000). The goat anti-rabbit and anti-mouse secondary antibodies were purchased from Proteintech. Shikonin (SK) was purchased from Med Chem Express and dissolved in DMSO.

Propidium Iodide (PI) /Hoechst staining

The cells were seeded in 96-well plates at 1×10^4 cells/well and treated with SK. Hoechst 33342 staining solution was added to each well and incubated for 30 min. Next, 5 μL of PI was added and observed under a fluorescence microscope (Olympus).

Cell viability assay

The cells were seeded in 96-well plates at a density of 1×10^4 cells/well. After treatment with SK at the indicated times, 10 μL of Cell Counting Kit-8 (CCK-8) reagent was added to each well, and the cells were incubated at 37 °C for 1 h in the dark. The absorbance was then detected at 450 nm.

LDH release assay

The supernatant of the treated cells was collected and transferred to a new 96-well plate. LDH reagent (Beyotime) was added, and the absorbance at 490 nm was detected by a microplate reader after incubation for 30 min.

Plasmid construction and lentivirus generation

The PLKO.1-shRNA recombinant plasmid was constructed as previously described to interfere with the expression of target genes [17]. The lentiviral vector and lentiviral packaging plasmid were mixed and transduced into HEK-293 FT cells using transfection reagent. The virus supernatant was collected 36 h

after transduction, the infected cells were selected by puromycin, and gene knockdown was verified by western blot.

Western blotting

The cells were lysed by RIPA (Beyotime) to collect total protein, and the protein concentration was determined by the BCA method before sample preparation. Total protein was separated by 10% SDS–PAGE and transferred to PVDF membranes. The membrane was then blocked for 1 h at room temperature in TBST containing 5% skim milk. The membrane was incubated with primary antibody at 4 °C overnight. After washing, the membrane was incubated with secondary antibody at room temperature for 1 h. Protein expression was visualized using a ChemiDoc XRS system (Bio-Rad, Hercules, CA, USA).

Fluorescence microscopy

The cells were transfected with PCDH-CMV-mRFP-GFP-hLC3B-EF1A-Puro plasmid and selected with puromycin to establish stable cell lines. The cells were then stimulated with SK at the indicated times. Subsequently, the cells were fixed with 4% paraformaldehyde at 37 °C for 10 min. After washing with PBS, the cells were observed under a laser confocal fluorescence microscope (Olympus).

Determination of intracellular ROS

Intracellular ROS levels were detected by the fluorescent probe 2,7-dichlorofluorescin diacetate (DCFH-DA, Beyotime). After treatment, the cells were incubated with diluted DCFH-DA at 37 °C for 20 min and then analysed by flow cytometry.

In vivo tumorigenesis assays

Female BALB/c mice were housed under pathogen-free conditions in the Animal Center of Jiangsu University. All animal experiments were approved by the Ethics Committee of Jiangsu University. A total of 1×10^6 EMT6 cells in 200 ml of PBS were subcutaneously (sc) injected into 6-week-old female BALB/c mice. When the tumours reached approximately 100 mm^3, the mice were randomly divided into two groups (n=9 per group). The experimental group mice were intraperitoneally injected with 2 mg/kg shikonin once every two days for a total of three injections. The control group was injected with PBS. The tumour size and weight were measured.

Statistical analysis

All of the data were analysed by GraphPad Prism 8. All group data are shown as the mean ± SD, and the difference between groups was analysed by t-test. $P<0.05$ indicates a statistically significant difference.

Results

Shikonin induced pyroptosis in tumour cells via GSDME

To investigate the anticancer effects of shikonin (SK), BGC and SGC cells were stimulated with SK. SK suppressed BGC and SGC cell proliferation in a time- and dose-dependent manner (Fig. 1A and Sup Fig. 1A and B). BGC and SGC cells stimulated with SK showed PI-positive staining and lactate dehydrogenase (LDH) release (Fig. 1A and Sup Fig. 1C). These cells showed typical morphological features of pyroptosis (Fig. 1B). Both GSDMD and GSDME are involved in pyroptotic pathways, and RIPK3 is involved in necroptotic pathways. We first investigated whether these molecules are involved in SK-induced cell death. GSDME knockdown significantly inhibited LDH release, whereas GSDMD or RIPK3 knockdown failed to inhibit LDH release (Fig. 1C). We then examined GSDME expression in several cancer cell lines. GSDME was highly expressed in SGC and BGC cells but not in AGS cells (Fig. 1D). SK treatment induced the cleavage of GSDME in SGC and BGC cells (Fig. 1E). In GSDME knockdown cells, SK stimulation led to an apoptotic morphology and less LDH release (Fig. 1F and G). GSDME cleavage was also abolished after GSDME knockdown (Fig. 1H). The overexpression of WT GSDME in AGS cells also induced GSDME cleavage and LDH release after SK stimulation (Sup Fig. 1D and E). Collectively, these results suggest that SK can induce pyroptosis in some tumour cells, and this induction is mediated by GSDME.

BAX/caspase-3 activation was involved in SK-induced pyroptosis

We next investigated the molecular mechanisms of the GSDME-mediated pyroptosis induced by SK. We pretreated cells with a pan-caspase inhibitor, Z-VAD-FMK, and then stimulated them with SK. Z-VAD-FMK treatment significantly prevented cell swelling (Fig. 2A), LDH release (Fig. 2B and C) and GSDME cleavage (Fig. 2B and C). These results suggest that caspase may be involved in GSDME-mediated pyroptosis. Previous studies have found that caspase-3 can cleave GSDME in GSDME-mediated pyroptosis [7]. To further clarify the essential role of caspase-3 in SK-induced pyroptosis, we knocked down caspase-3 in SGC and BGC cells. As shown in Fig. 2D and E, caspase-3 knockdown significantly prevented cell death and reduced GSDME cleavage. BAX activation led to pore formation on the mitochondrial outer membrane, which would induce the activation of the caspase cascade [18]. We then investigated whether BAX activation induces caspase-3 cleavage and is involved in SK-induced pyroptosis. After BAX knockdown (Sup Fig. 2A), both caspase-3 and GSDME cleavage were reduced compared with the control (Fig. 2F). LDH release was also diminished in BAX-knockdown cells (Fig. 2F). Taken together, these data indicated that SK treatment activated the BAX/caspase-3/GSDME cascade to induce pyroptosis.

SK induced protective autophagy in tumour cells

It has been reported that some natural compounds can modulate crosstalk between apoptosis and autophagy [19]. However, it is unknown whether there is crosstalk between pyroptosis and autophagy after SK stimulation. We first examined the expression level of LC3-II, an important marker of autophagosomes, by western blotting. As shown in Fig. 3A, after SK stimulation, the LC3-II expression level was markedly increased in a time-dependent manner. We further examined autophagic flux by transducing mRFP-GFP-LC3 lentivirus into cells. SK stimulation increased the number of red puncta

(autophagolysosomes) (Fig. 3B), indicating that SK stimulation promotes autophagic flux. Next, we investigated whether SK-induced autophagy affected GSDME-mediated pyroptosis. Beclin-1 and ATG5, key molecular regulators of autophagy, were knocked down in cells by shRNA (Sup Fig. 3A and 3B). SK stimulation markedly increased the change in pyroptotic morphology (Fig. 3C), cell death (Fig. 3D, G and Sup Fig. 3D), caspase-3 and GSDME cleavage compared with the control group (Fig. 3E, F and Sup Fig. 3C). Collectively, these findings demonstrated that autophagy exerts cytoprotective effects in SK-induced pyroptosis.

SK induced pyroptosis and autophagy through ROS-initiated signalling

SK stimulation can reportedly induce cell death via the generation of ROS in some tumour cells [20]. However, whether SK-elevated ROS generation is associated with GSDME-mediated pyroptosis is still unknown. We first measured the ROS levels in tumour cells after SK treatment. SK treatment significantly increased ROS levels in cells (Fig. 4A). Importantly, treatment with NAC, a ROS scavenger, dramatically reduced ROS production in SK-treated cells (Fig. 4A). Moreover, NAC treatment also markedly attenuated cell death (Fig. 4B), the change in pyroptotic morphology (Fig. 4C), caspase-3 and GSDME cleavage compared with the control (Fig. 4D). We further investigated whether ROS generation in SK-treated cells was affected by caspase-3 and GSDME. As shown in Fig. 4E and F, SK-induced ROS generation was not affected in caspase-3- or GSDME-knockdown cells compared with the control groups. This result suggested that ROS are upstream signals of caspase-3 and GSDME. Taken together, these data indicate that SK induces pyroptosis through ROS-initiated signalling to activate caspase-3 and GSDME.

The regulation of autophagy by ROS has been observed in cancer cells, and autophagy, in turn, can reduce oxidative damage [4]. However, whether SK-induced protective autophagy is also regulated by ROS is still unknown. We first treated cells with NAC and examined LC3-II expression and autophagic flux after SK treatment. The NAC-treated cells showed lower LC3-II expression than the control cells (Fig. 4G). The number of red puncta was also reduced in the NAC-treated cells (Fig. 4G). Collectively, these results suggest that SK-induced ROS generation also regulates autophagy and ultimately affects GSDME-mediated pyroptosis.

MAPK14/p38α-dependent modulation of SK-induced autophagy and pyroptosis in SK-induced pyroptosis

To identify the potential factors that regulate GSDME-mediated pyroptosis in SK-treated cells, we performed a high-sensitivity mass spectrometry assay that compared SK-treated cells and control cells. The differentially expressed proteins between SK-treated cells and control cells that are involved in cell death and autophagy are shown in Fig. 5A. One of the proteins, MAPK14, showed significantly decreased expression in the SK-treated group. MAPK14 was previously found to be a stress-activated protein kinase that can sense ROS and affect autophagy [21, 22]. We then investigated whether MAPK14 was involved in SK-induced pyroptosis and autophagy. In MAPK14-knockdown cells (Sup Fig. 4A), the number of red puncta and LC3-II expression were increased after SK treatment (Fig. 5B, C and E), suggesting that MAPK14 modulates autophagy. Next, we examined whether MAPK14 affects GSDME

cleavage and pyroptosis. In MAPK14-knockdown cells, cell viability was increased compared with control cells after SK treatment (Fig. 5D). Caspase-3 and GSDME cleavage were also reduced in MAPK14-knockdown cells (Fig. 5E). Taken together, these data indicated that MAPK14 modulates SK-induced autophagy and eventually affects pyroptosis.

SK treatment decreased tumorigenicity and induced GSDME-mediated pyroptosis in vivo

Next, we sought to investigate the effect of SK administration on tumour growth in vivo by using a mouse model. We first examined whether SK treatment induces GSDME-mediated pyroptosis in a mouse cell line. EMT6 cells, which highly express GSDME, were used to analyse cell death and GSDME cleavage [7]. SK treatment significantly induced caspase-3, GSDME cleavage, and cell death in EMT6 cells (Fig. 6A and B). However, in GSDME-knockdown cells (Sup Fig. 4B), caspase-3, GSDME cleavage, and cell death were reduced compared with the control cells. Next, we ascertained the effect of SK on the growth of xenografts in immune-competent BALB/c mice. As shown in Figure 6C, SK administration significantly inhibited the growth of EMT6 solid tumours from Day 17. Moreover, the tumour volume and weight of SK-treated mice were significantly lower than those of the control mice (Fig. 6D and E). Immunohistochemical analysis of the xenografts showed that SK administration significantly enhanced the expression of caspase-3 and GSDME (Fig. 6F and G). Collectively, these results suggested that SK inhibits the growth of tumours in vivo by inducing pyroptosis.

Discussion

Several anticancer drugs have been derived from natural products; these drugs have unique advantages over other chemotherapy drugs, such as having lower toxicity [23]. Many of these natural products inhibit tumour growth by inducing apoptosis; however, some tumours become resistant to apoptosis. Therefore, there is an urgent need to find drugs that can induce other types of tumour cell death [24]. Recent studies have found that many natural products can also induce pyroptosis in tumour cells to inhibit tumour growth [10, 25, 26]. In this study, we found that SK induces pyroptosis in tumour cells instead of apoptosis or necroptosis (Fig. 1). Previous studies have shown that SK can induce apoptosis or necroptosis in some tumour cells [27, 28]. However, we found that SK induced pyroptosis but not apoptosis or necroptosis. SK might induce pyroptosis in these cells because of their high expression levels of GSDME. We also found that AGS cells that do not express GSDME can undergo pyroptosis when GSDME is overexpressed in the cells (Sup Fig. 1). In contrast, in GSDME-knockdown BGC cells, the cells underwent apoptosis instead of pyroptosis (Fig. 1). These results are consistent with a previous study that showed that GSDME can switch caspase-3-mediated apoptosis [7]. The BAX-dependent mitochondrial pathway to activate caspase-3 cleavage is reportedly involved in the pyroptosis pathway [18]. We also found that activation of BAX/caspase-3 was involved in SK-induced pyroptosis (Fig. 2).

Accumulating data suggest that ROS have an essential role in cell death and autophagy [29]. ROS play a dual role in tumour cells. Low levels of ROS can promote tumour growth; however, the continuous release of ROS can induce tumour cell death. Several natural products have been reported to induce cell death by

inducing ROS production [9, 10]. We also observed that SK stimulation induced ROS production in cells. Furthermore, NAC, a ROS scavenger, significantly inhibited SK-induced pyroptosis. ROS acted as upstream signals of caspase-3 and GSDME (Fig. 4). These results are consistent with previous studies showing that ROS can initiate cell death in tumour cells [5, 20]. Autophagy also plays a dual role in the different tumour stages; it inhibits tumour formation in the early stage of tumour development and promotes tumour growth in the later stages [20]. We observed that SK treatment induced autophagy (Fig. 3). Interestingly, we revealed that pyroptosis was increased when autophagy was inhibited, suggesting that autophagy plays a role in protecting tumour cells during SK stimulation (Fig. 3). It is generally believed that increased intracellular ROS promotes autophagy [30]. Our results demonstrated that ROS generation after SK stimulation regulated autophagy and, in turn, affected pyroptosis (Fig. 5). MAPK14 pathways reportedly regulate the balance between cell death and autophagy [31]. MAPK14 was also reported as a sensor of ROS in tumorigenesis [22]. Through high-throughput screening, we found that MAPK14 can also regulate autophagy and pyroptosis (Fig. 5).

Our in vivo study further supported the finding that SK stimulation induced GSDME-mediated pyroptosis. Importantly, we found that SK stimulation induced GSDME-mediated pyroptosis in mouse cells. Low-dose SK treatment significantly inhibited tumour growth in mice (Fig. 6). Collectively, these results suggest that SK has potential as a natural product to kill tumour cells by inducing tumour cell death through pyroptosis.

Declarations

Funding

This work was supported by the National Natural Science Foundation of China (81502621) and key research and development program of Zhenjiang (SH2021058)

Contributions

Xiaoli Ju: Conceptualization, Methodology, Software **Jiayou Wang**: Data curation, Writing- Original draft preparation. **Jin Wang and Lanfang Guo**: Visualization, Investigation. **Heng Zhang and Qiang Wang***:* Supervision Writing- Reviewing and Editing

Ethics approval

All of the animal experiments were approved by the Animal Research Committee of JiangSu University. Animal research was conducted in accordance with international guidelines.

Conflict of interest

The authors declare no competing interests.

References

1. J.N. Moloney, T.G. Cotter, ROS signalling in the biology of cancer, Semin Cell Dev Biol 80 (2018) 50–64.
2. S.J. Dixon, B.R. Stockwell, The role of iron and reactive oxygen species in cell death, Nat Chem Biol 10(1) (2014) 9–17.
3. J. Zhang, D. Duan, Z.L. Song, T. Liu, Y. Hou, J. Fang, Small molecules regulating reactive oxygen species homeostasis for cancer therapy, Med Res Rev 41(1) (2021) 342–394.
4. L. Poillet-Perez, G. Despouy, R. Delage-Mourroux, M. Boyer-Guittaut, Interplay between ROS and autophagy in cancer cells, from tumor initiation to cancer therapy, Redox Biol 4 (2015) 184–92.
5. J.Z. Liu, Y.L. Hu, Y. Feng, Y. Jiang, Y.B. Guo, Y.F. Liu, X. Chen, J.L. Yang, Y.Y. Chen, Q.S. Mao, W.J. Xue, BDH2 triggers ROS-induced cell death and autophagy by promoting Nrf2 ubiquitination in gastric cancer, J Exp Clin Cancer Res 39(1) (2020) 123.
6. X. Ju, Z. Yang, H. Zhang, Q. Wang, Role of pyroptosis in cancer cells and clinical applications, Biochimie 185 (2021) 78–86.
7. Y. Wang, W. Gao, X. Shi, J. Ding, W. Liu, H. He, K. Wang, F. Shao, Chemotherapy drugs induce pyroptosis through caspase-3 cleavage of a gasdermin, Nature 547(7661) (2017) 99–103.
8. Z. Zhang, Y. Zhang, S. Xia, Q. Kong, S. Li, X. Liu, C. Junqueira, K.F. Meza-Sosa, T.M.Y. Mok, J. Ansara, S. Sengupta, Y. Yao, H. Wu, J. Lieberman, Gasdermin E suppresses tumour growth by activating anti-tumour immunity, Nature 579(7799) (2020) 415–420.
9. X. Zhang, P. Zhang, L. An, N. Sun, L. Peng, W. Tang, D. Ma, J. Chen, Miltirone induces cell death in hepatocellular carcinoma cell through GSDME-dependent pyroptosis, Acta Pharm Sin B 10(8) (2020) 1397–1413.
10. J. Cai, M. Yi, Y. Tan, X. Li, G. Li, Z. Zeng, W. Xiong, B. Xiang, Natural product triptolide induces GSDME-mediated pyroptosis in head and neck cancer through suppressing mitochondrial hexokinase-Iotalota, J Exp Clin Cancer Res 40(1) (2021) 190.
11. R. Zhang, J. Chen, L. Mao, Y. Guo, Y. Hao, Y. Deng, X. Han, Q. Li, W. Liao, M. Yuan, Nobiletin Triggers Reactive Oxygen Species-Mediated Pyroptosis through Regulating Autophagy in Ovarian Cancer Cells, J Agric Food Chem 68(5) (2020) 1326–1336.
12. Z. Liu, Y. Li, Y. Zhu, N. Li, W. Li, C. Shang, G. Song, S. Li, J. Cong, T. Li, Z. Xiu, J. Lu, C. Ge, X. Yang, Y. Li, L. Sun, X. Li, N. Jin, Apoptin induces pyroptosis of colorectal cancer cells via the GSDME-dependent pathway, Int J Biol Sci 18(2) (2022) 717–730.
13. Y. Xiao, T. Zhang, X. Ma, Q.C. Yang, L.L. Yang, S.C. Yang, M. Liang, Z. Xu, Z.J. Sun, Microenvironment-Responsive Prodrug-Induced Pyroptosis Boosts Cancer Immunotherapy, Adv Sci (Weinh) 8(24) (2021) e2101840.
14. B. Zhou, J.Y. Zhang, X.S. Liu, H.Z. Chen, Y.L. Ai, K. Cheng, R.Y. Sun, D. Zhou, J. Han, Q. Wu, Tom20 senses iron-activated ROS signaling to promote melanoma cell pyroptosis, Cell Res 28(12) (2018) 1171–1185.
15. Q. Wang, J. Wang, J. Wang, X. Ju, H. Zhang, Molecular mechanism of shikonin inhibiting tumor growth and potential application in cancer treatment, Toxicol Res (Camb) 10(6) (2021) 1077–1084.

16. Q. Sun, T. Gong, M. Liu, S. Ren, H. Yang, S. Zeng, H. Zhao, L. Chen, T. Ming, X. Meng, H. Xu, Shikonin, a naphthalene ingredient: Therapeutic actions, pharmacokinetics, toxicology, clinical trials and pharmaceutical researches, Phytomedicine 94 (2022) 153805.
17. X. Ju, H. Zhang, Z. Zhou, M. Chen, Q. Wang, Tumor-associated macrophages induce PD-L1 expression in gastric cancer cells through IL-6 and TNF-a signaling, Experimental cell research 396(2) (2020) 112315.
18. L. Hu, M. Chen, X. Chen, C. Zhao, Z. Fang, H. Wang, H. Dai, Chemotherapy-induced pyroptosis is mediated by BAK/BAX-caspase-3-GSDME pathway and inhibited by 2-bromopalmitate, Cell death & disease 11(4) (2020) 281.
19. C. Braicu, O. Zanoaga, A.A. Zimta, A.B. Tigu, K.L. Kilpatrick, A. Bishayee, S.M. Nabavi, I. Berindan-Neagoe, Natural compounds modulate the crosstalk between apoptosis- and autophagy-regulated signaling pathways: Controlling the uncontrolled expansion of tumor cells, Semin Cancer Biol 80 (2022) 218–236.
20. M.F. Tsai, S.M. Chen, A.Z. Ong, Y.H. Chung, P.N. Chen, Y.H. Hsieh, Y.T. Kang, L.S. Hsu, Shikonin Induced Program Cell Death through Generation of Reactive Oxygen Species in Renal Cancer Cells, Antioxidants (Basel) 10(11) (2021).
21. E. Desideri, R. Vegliante, S. Cardaci, R. Nepravishta, M. Paci, M.R. Ciriolo, MAPK14/p38alpha-dependent modulation of glucose metabolism affects ROS levels and autophagy during starvation, Autophagy 10(9) (2014) 1652–65.
22. I. Dolado, A. Swat, N. Ajenjo, G. De Vita, A. Cuadrado, A.R. Nebreda, p38alpha MAP kinase as a sensor of reactive oxygen species in tumorigenesis, Cancer Cell 11(2) (2007) 191–205.
23. A.G. Atanasov, S.B. Zotchev, V.M. Dirsch, T. International Natural Product Sciences, C.T. Supuran, Natural products in drug discovery: advances and opportunities, Nat Rev Drug Discov 20(3) (2021) 200–216.
24. J. Ye, R. Zhang, F. Wu, L. Zhai, K. Wang, M. Xiao, T. Xie, X. Sui, Non-apoptotic cell death in malignant tumor cells and natural compounds, Cancer Lett 420 (2018) 210–227.
25. F. Zhang, Q. Liu, K. Ganesan, Z. Kewu, J. Shen, F. Gang, X. Luo, J. Chen, The Antitriple Negative Breast cancer Efficacy of Spatholobus suberectus Dunn on ROS-Induced Noncanonical Inflammasome Pyroptotic Pathway, Oxid Med Cell Longev 2021 (2021) 5187569.
26. Q. Li, L. Chen, Z. Dong, Y. Zhao, H. Deng, J. Wu, X. Wu, W. Li, Piperlongumine analogue L50377 induces pyroptosis via ROS mediated NF-kappaB suppression in non-small-cell lung cancer, Chem Biol Interact 313 (2019) 108820.
27. Y. Nie, Y. Yang, J. Zhang, G. Cai, Y. Chang, G. Chai, C. Guo, Shikonin suppresses pulmonary fibroblasts proliferation and activation by regulating Akt and p38 MAPK signaling pathways, Biomed Pharmacother 95 (2017) 1119–1128.
28. B. Lu, X. Gong, Z.Q. Wang, Y. Ding, C. Wang, T.F. Luo, M.H. Piao, F.K. Meng, G.F. Chi, Y.N. Luo, P.F. Ge, Shikonin induces glioma cell necroptosis in vitro by ROS overproduction and promoting RIP1/RIP3 necrosome formation, Acta Pharmacol Sin 38(11) (2017) 1543–1553.

29. A.Q. Khan, K. Rashid, A.A. AlAmodi, M.V. Agha, S. Akhtar, I. Hakeem, S.S. Raza, S. Uddin, Reactive oxygen species (ROS) in cancer pathogenesis and therapy: An update on the role of ROS in anticancer action of benzophenanthridine alkaloids, Biomed Pharmacother 143 (2021) 112142.
30. R. Scherz-Shouval, Z. Elazar, Regulation of autophagy by ROS: physiology and pathology, Trends Biochem Sci 36(1) (2011) 30–8.
31. X. Sui, N. Kong, L. Ye, W. Han, J. Zhou, Q. Zhang, C. He, H. Pan, p38 and JNK MAPK pathways control the balance of apoptosis and autophagy in response to chemotherapeutic agents, Cancer Lett 344(2) (2014) 174–9.

Figures

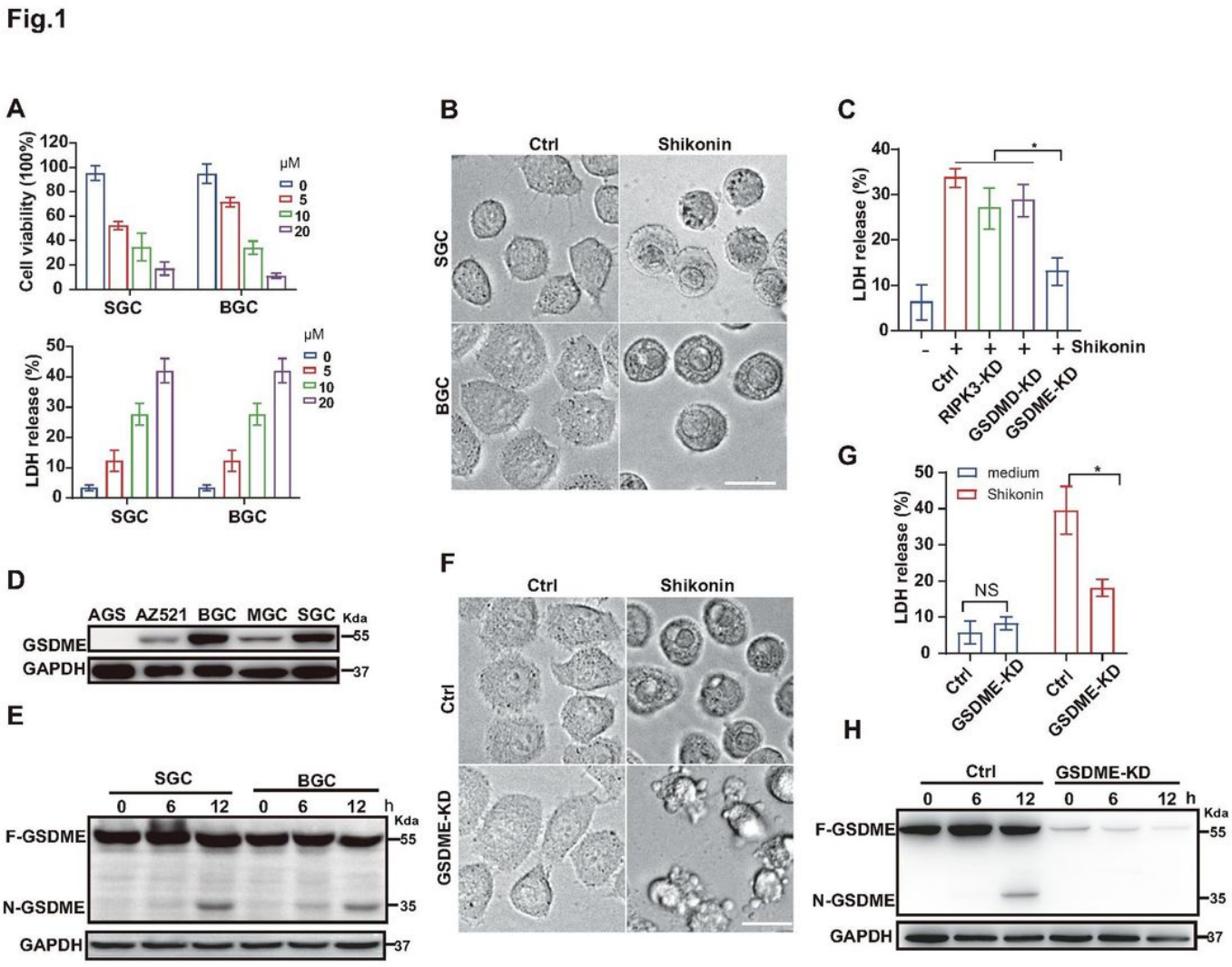

Figure 1

Shikonin induced GSDME-mediated pyroptosis in human tumour cells. A and B. SGC and BGS cells were treated with 0-20 μM SK for 12 h. Cell viability was determined by CCK-8 assay. LDH release was

measured (A), and cell morphology was observed under bright-field microscopy (B). Scale bar, 20 μm. C. Control, RIPK3-KD, GSDMD-KD or GSDME-KD cells were treated with 20 μM SK for 12 h, and LDH release was measured. KD: knockdown. Ctrl: control. D. The expression of endogenous GSDME in the indicated cell lines was determined by western blotting. E. SGC and BGS cells were treated with 20 μM SK for 6 or 12 h. GSDME cleavage was determined by western blotting. F-H. Control or GSDME-KD cells were treated with 20 μM SK for 6 or 12 h. Cell morphology was observed (F), LDH release was measured (G), and GSDME cleavage was determined by western blotting (H). Scale bar, 20 μm. *P < 0.05.

Fig.2

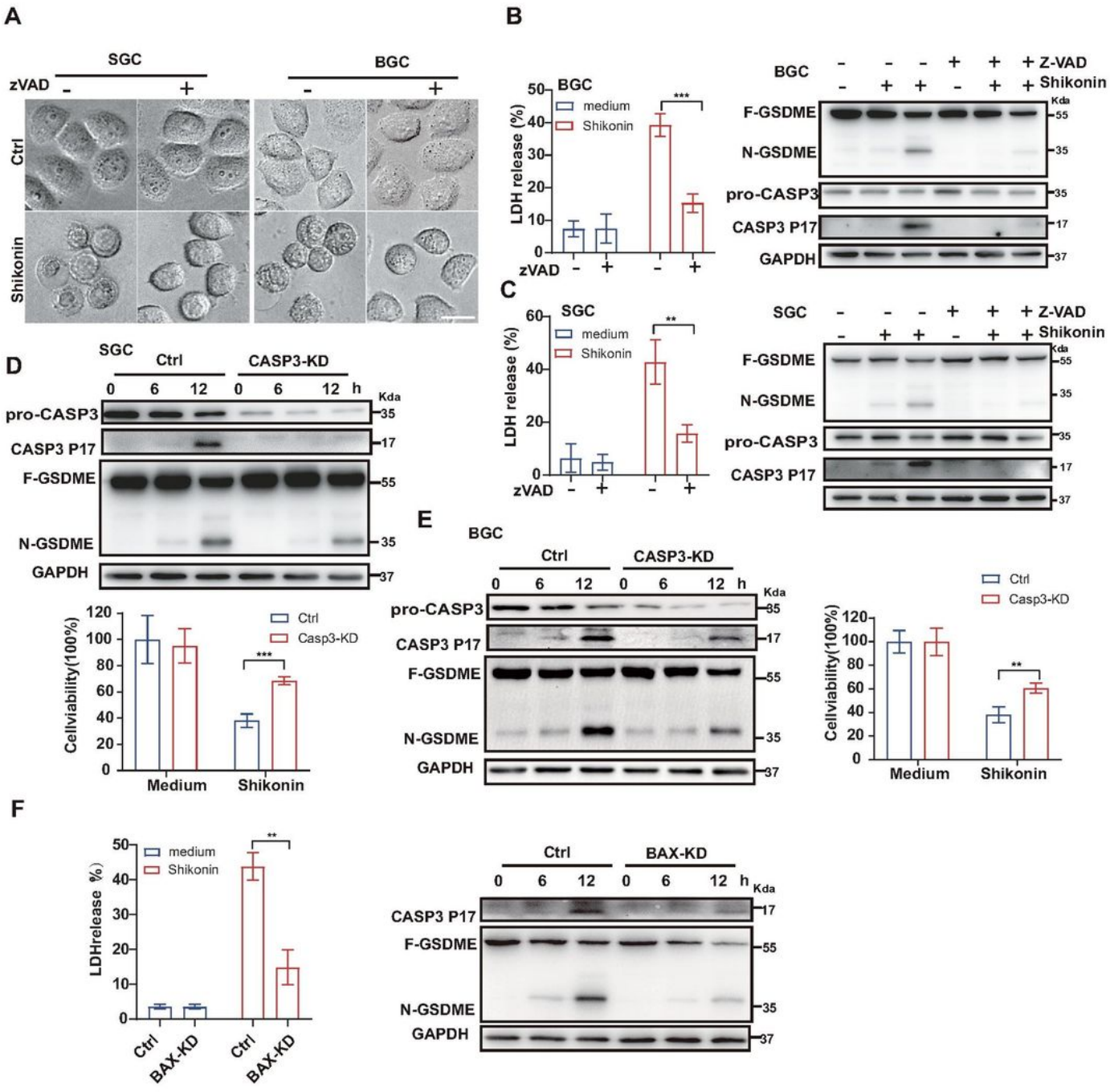

Figure 2

Activation of the BAX/caspase-3 pathway triggered GSDME-mediated pyroptosis after shikonin treatment. A-C. SGC and BGS cells were pretreated with 20 μM zVAD for 1 h and then stimulated with 20 μM SK for 12 h. Cell morphology was observed (A), LDH release was measured and GSDME cleavage was determined by western blotting (B and C). Scale bar, 20 μm. D and E. Ctrl and CASP3-KD cells were treated with 20 μM SK for 6 or 12 h. Cell viability was determined by CCK-8 assay, and CASP3 and GSDME cleavage was determined by western blotting. CASP3-KD: Caspase-3 knockdown. F. Ctrl and BAX-KD cells were treated with 20 μM SK for 6 or 12 h. LDH release was measured, and CASP3 and GSDME cleavage was determined by western blotting. KD: knockdown. Ctrl: control. **P < 0.01, ***P < 0.001.

Fig.3

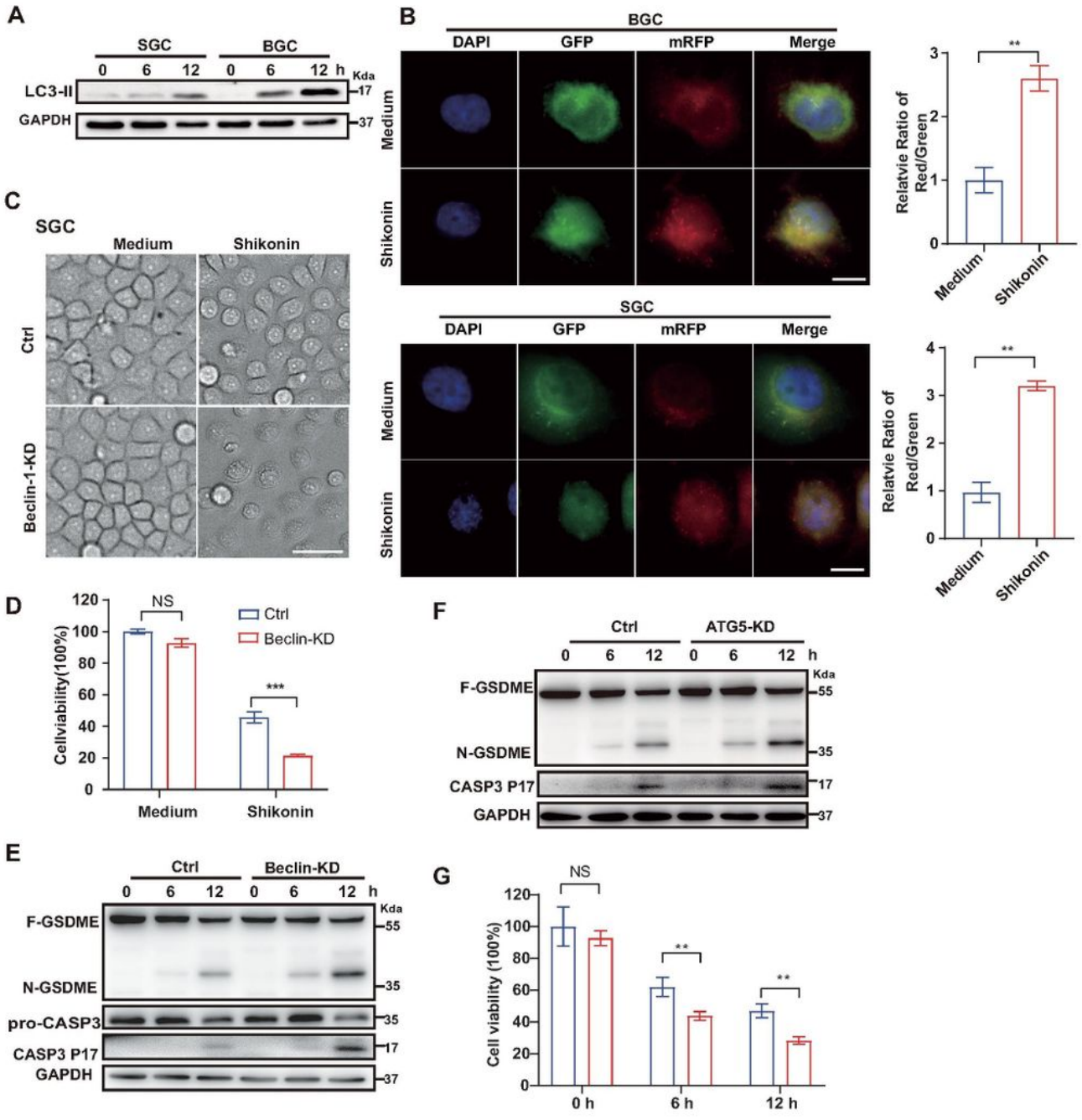

Figure 3

Shikonin treatment induced protective autophagy in human tumour cells. A. SGC and BGS cells were treated with 20 μM SK for 6 or 12 h. LC3-II expression levels were detected by western blotting. B. BGC and SGC cells expressing mRFP-GFP-LC3B were treated with 20 μM SK for 6 h. Nuclei were stained with DAPI, and the cells were visualized by confocal microscopy. The average number of autophagosomes (yellow puncta) and autolysosomes (red puncta) per detected cell was calculated. Scale bar: 10 μm. D-G.

Ctrl, Beclin-KD (D and E) and ATG5-KD (F and G) cells were treated with 20 μM SK for 6 or 12 h. Cell viability was determined by CCK-8 assay (D and G). LDH release was measured (G), and CASP3 and GSDME cleavage were determined by western blotting (E and F). KD: knockdown. Ctrl: control. **P < 0.01, ***P < 0.001.

Fig.4

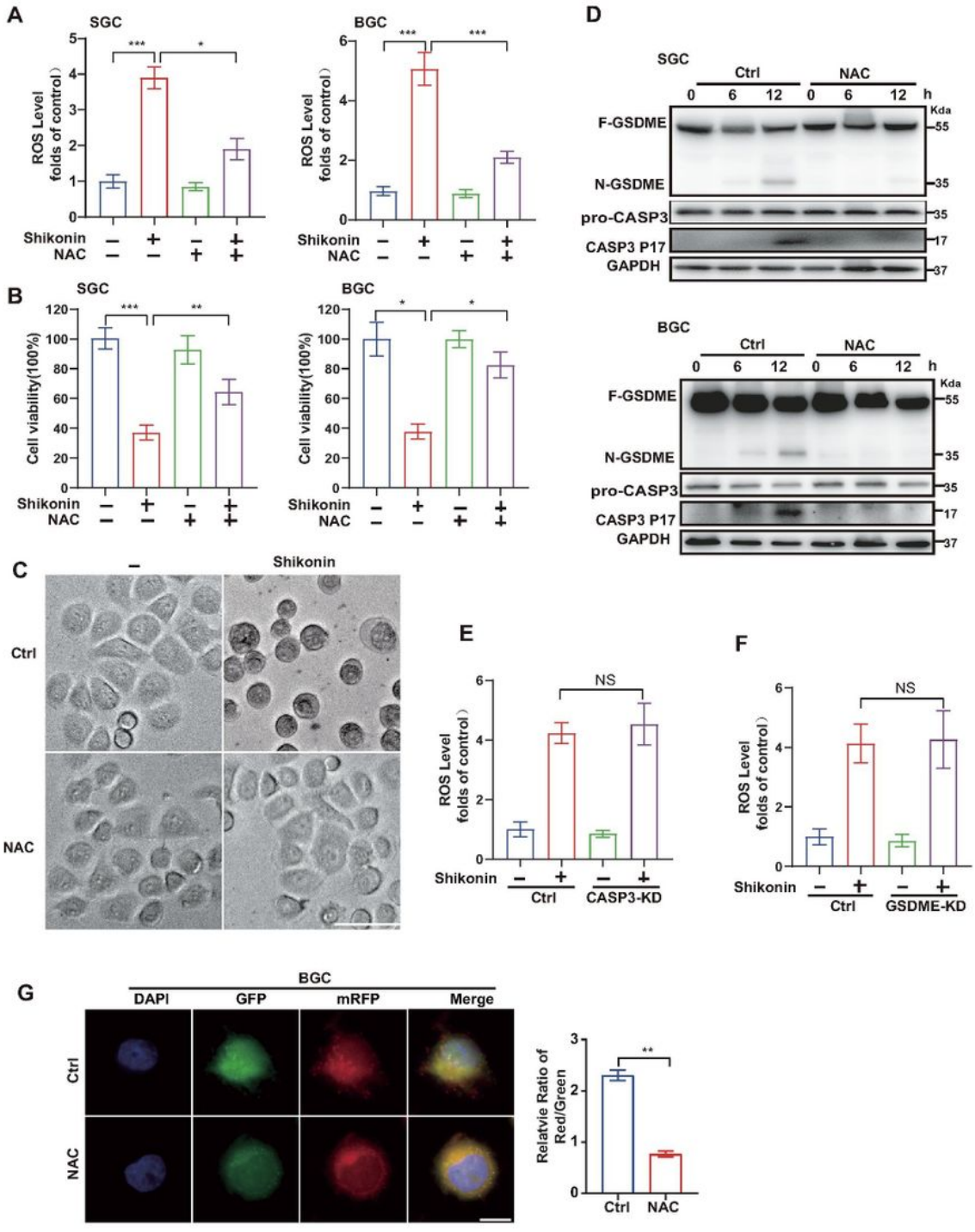

Figure 4

ROS generation initiated shikonin-induced autophagy and pyroptosis. A-D. SGC and BGS cells were pretreated with 5 mM NAC for 1 h and then stimulated with 20 μM SK for 12 h. ROS levels were detected (A); cell viability was determined by CCK-8 assay (B); cell morphology was observed (C); CASP3 expression and GSDME cleavage were determined by western blotting (D). Scale bar, 20 μm. E and F. Ctrl, CASP3-KD and GSDME-KD cells were treated with 20 μM SK for 6 or 12 h, and the ROS levels were then detected. G. BGS cells were pretreated with 5 mM NAC for 1 h and then stimulated with 20 μM SK for 12 h. Cells were visualized by confocal microscopy. Scale bar, 20 μm. *P < 0.05, **P < 0.01, ***P < 0.001.

Fig.5

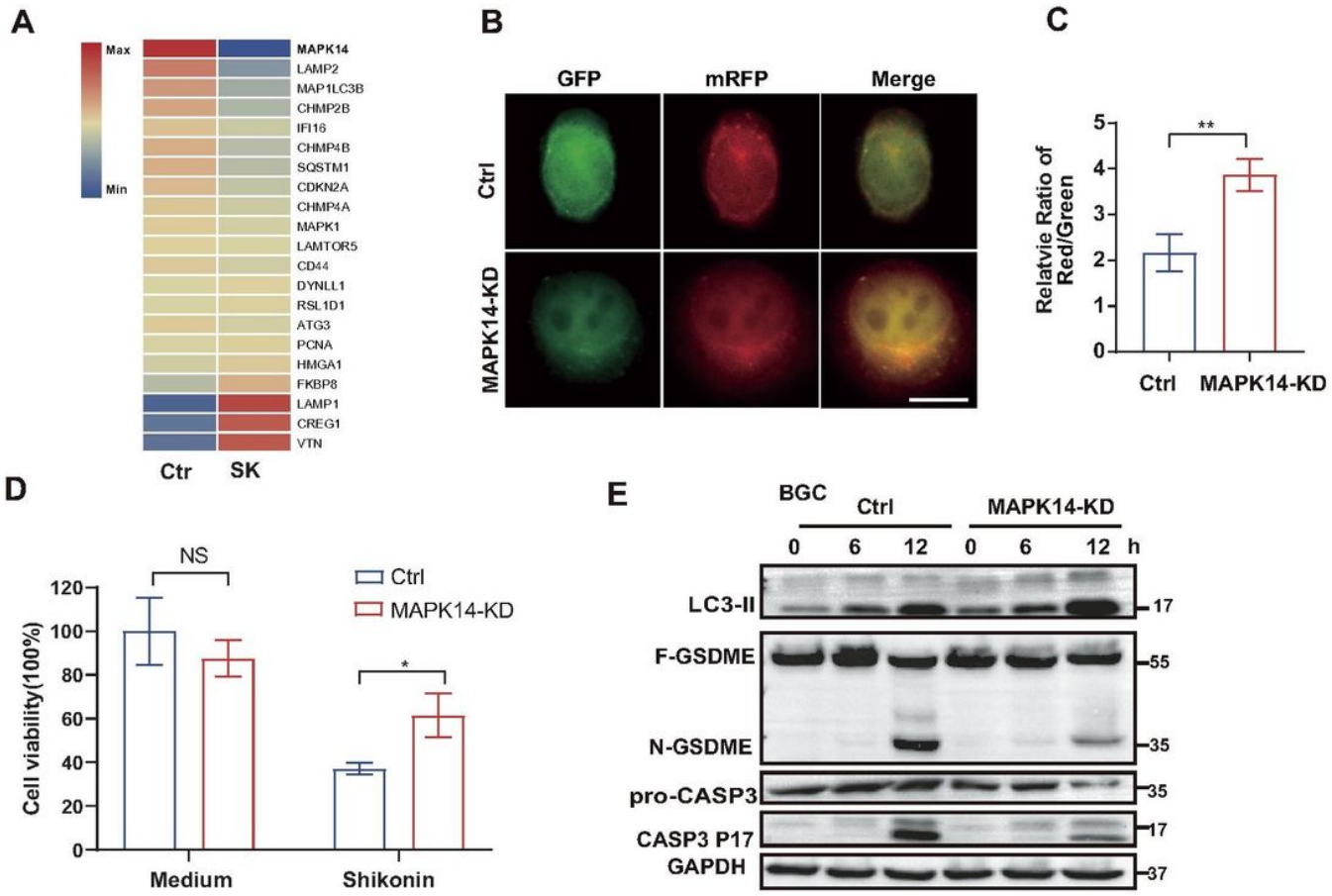

Figure 5

MAPK14/p38α contributed to shikonin-induced autophagy and pyroptosis. A. Differentially expressed proteins between SK-treated cells and control cells by high-sensitivity mass spectrometry assay. B and C. Ctrl and MAPK14-KD cells expressing mRFP-GFP-LC3B were treated with 20 μM SK for 6 h, and the cells were visualized by confocal microscopy (B). The average number of autophagosomes (yellow puncta) and autolysosomes (red puncta) per detected cell was calculated (C). Scale bar: 10 μm. D and E. Control and MAPK14-KD cells were treated with 20 μM SK for 6 or 12 h, and cell viability was determined by CCK-

8 assay (D). The expression levels of LC3-II, CASP3 and GSDME cleavage were determined by western blotting (E). KD: knockdown. Ctrl: control. *P < 0.05, **P < 0.01.

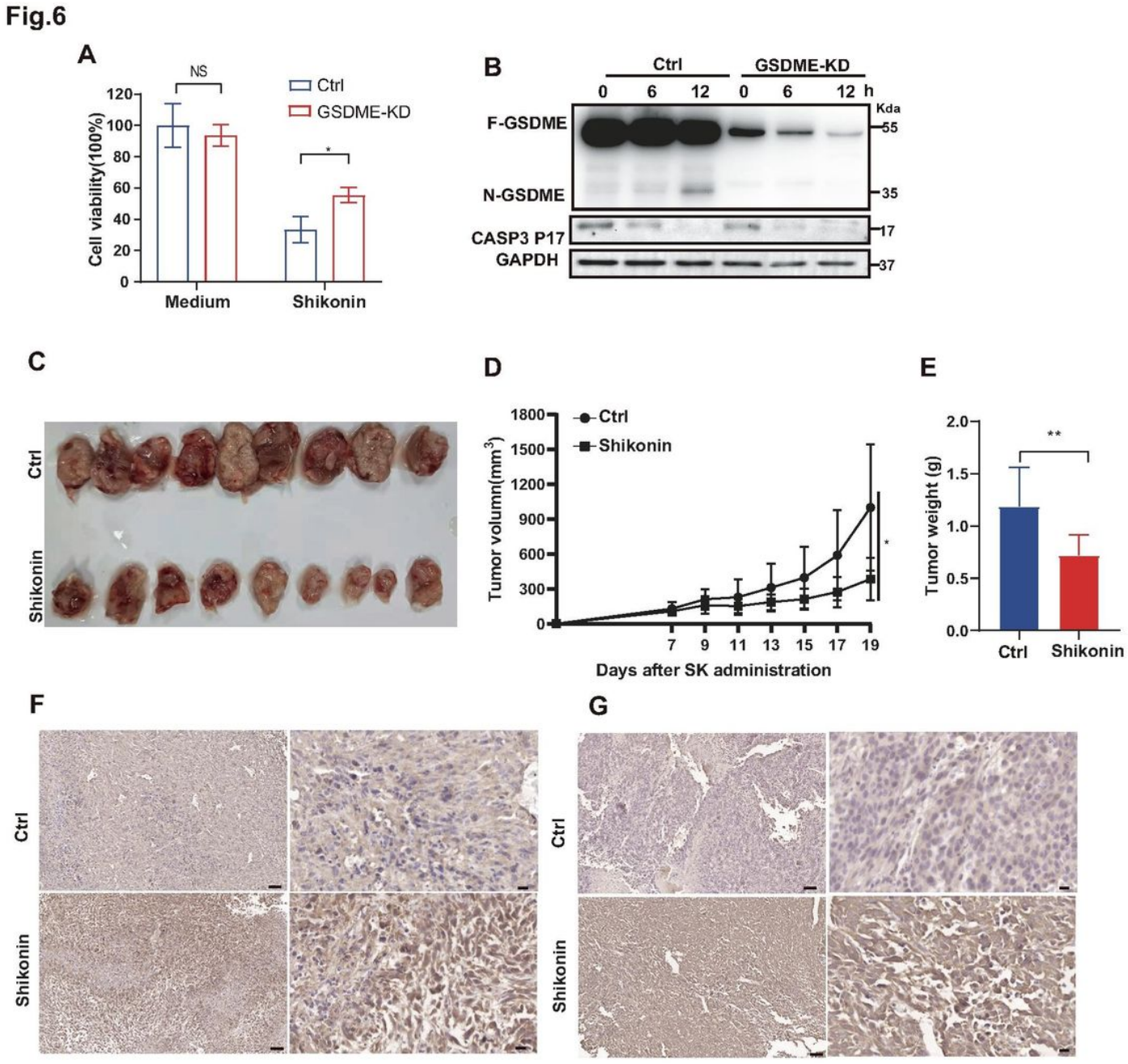

Figure 6

Shikonin inhibited tumour growth in vivo through GSDME-mediated pyroptosis. A and B. Mouse EMT6 cells were stimulated with 10 μM SK for 6 or 12 h. Cell viability was determined by CCK-8 assay (A). CASP3 and GSDME cleavage were determined by western blotting (B). C-E. EMT6 cells were subcutaneously injected into 6-week-old female BALB/c mice. The mice were then treated with PBS (Ctrl) or shikonin. Images of each group of tumours are from the same day (the endpoint of the experiment)

(C). Tumour volumes were measured every other day of treatment (D). Tumour weights in each group were measured at the endpoint of the experiment (E). F and G.

The levels of GSDME (F) and caspase-3 (G) were examined by immunohistochemical staining. Scale bar: 100 μm for original magnification × 100; 20 μm for original magnification × 400. *P < 0.05, **P < 0.01.

Supplementary Files

This is a list of supplementary files associated with this preprint. Click to download.

- figS1S2.jpg
- figS3S4.jpg